



Contents lists available at ScienceDirect

Tetrahedron

journal homepage: www.elsevier.com/locate/tet

Synthesis and optical and electrochemical properties of a bispyrimidinium-dibenzothiophene-*S,S*-dioxide-based cationic conjugated polymer

Guiting Chen, Wei Yang, Bin Zhang*

Institute of Polymer Optoelectronic Materials and Devices, State Key Laboratory of Luminescent Materials and Devices, South China University of Technology, Guangzhou 510640, China

ARTICLE INFO

Article history:

Received 18 January 2017

Received in revised form

15 March 2017

Accepted 20 March 2017

Available online xxx

Keywords:

Dibenzothiophene-*S,S*-dioxide

Pyrimidinium

n-type

Polyelectrolyte

Conjugated polymer

ABSTRACT

A novel n-type cationic conjugated polymer (**PFSOmiCl**), consisting of bispyrimidinium-dibenzothiophene-*S,S*-dioxide and fluorene scaffolds, was developed from its polymeric precursor (**PFSOmi**) through an intramolecular cyclization reaction. In comparison with **PFSOmi**, **PFSOmiCl** exhibits significant bathochromical absorption and photoluminescence spectra in both solution and film form, as well as a more hydrophilic film surface. Cyclic voltammetry tests demonstrate that **PFSOmiCl** possesses a deep lowest unoccupied molecular orbital (LUMO) energy level of -4.18 eV, which is comparable to the LUMO energy levels of common fullerene derivatives. These unique properties endow **PFSOmiCl** with great utilization potential in organic optoelectronic devices. Moreover, this research offers a novel guideline for designing new conjugated polyelectrolytes.

© 2017 Elsevier Ltd. All rights reserved.

1. Introduction

Conjugated polymers have been widely used in organic electronic devices, such as organic light-emitting diodes (OLEDs),^{1–3} organic photovoltaics (OPVs),^{4–6} organic field-effect transistors^{7–9} and bio/chemosensors,^{10,11} as a result of their significant advantages, including light weight, low cost, flexibility and large-scale solution processing. In comparison with the rapid development of p-type (hole-transporting) conjugated polymers,^{12–14} the lack of high-performance n-type (electron-transporting) polymeric semiconductors has significantly hindered the improvement in performance of organic photoelectric devices. For instance, as only a small amount of n-type conjugated polymers and small molecules can adequately serve as electron acceptors in OPVs,^{15–17} researchers have been forced to use high-cost fullerene derivatives as acceptors in order to improve efficiencies.¹⁸ Alternatively, in the bio/chemosensor field, investigations have been mainly focused on synthesizing electron-donating polymers to detect electron-deficient analytes.^{19–22} However, reports of electron-withdrawing polymers for the detection of electron-rich analytes are not in

abundance.^{23–25}

In past decades, water/alcohol-soluble conjugated polymers (WSCPs) have attracted significant attention and been extensively utilized in OLEDs,^{26,27} OPVs^{28,29} and bio/chemosensors.³⁰ By incorporating surfactant-like polar groups (e.g., ammonium,^{31,32} sulfonate and³³ phosphonate groups³⁴), conjugated polymers can be dissolved in highly polar solvents, such as water, dimethyl sulfoxide (DMSO), methanol and so on. This kind of unusual solubility offers an opportunity to fabricate multilayer optoelectronic devices via orthogonal solvent processing techniques without interfacial erosion problems, when WSCPs are used as electrode interfacial layers in OLEDs and OPVs.^{27,28} In addition, solubility in aqueous media, which is an essential property for biosensors, makes WSCPs capable of interacting with biomacromolecules that are only soluble in aqueous solution.³⁰ However, most of the reported WSCPs are based on electron-rich backbones, and ideally, n-type WSCPs with electron-deficient backbones are more efficient for electron transportation and extraction in organic electronic devices.³⁵ Hence, it is necessary to develop new n-type WSCPs to improve the performance of OPVs, OLEDs and perovskite solar cells (PVSCs), as well as to detect electron-donating analytes.

Recently, the Swager group synthesized a series of cationic conjugated polymers composed of bispyridinium-phenylene

* Corresponding author.

E-mail address: msbzhang@scut.edu.cn (B. Zhang).

scaffolds that showed high electron affinities and conductivities.^{24,25,36–38} Because of their significant electron-withdrawing abilities, some of these WSCPs exhibited admirable sensing performance when they were used to detect electron-donating analytes (e.g., volatile amines and caffeine).^{24,25} Su and co-workers prepared three n-type conjugated small molecules containing bispyridinium–phenylene units, and used one of them for improving the cathode interfacial contact of an OPV.³⁹ Interestingly, they found that their material could create an interfacial dipole between the active layer and metal cathode, which was consistent with the research of Kim and co-workers.⁴⁰ This dipole could reduce the work function of cathode and thus increase the built-in potential across the device. As a result, the short-circuit current (J_{sc}), open-circuit voltage (V_{oc}) and fill factor (FF) of the OPV were simultaneously enhanced. Based on the above results, cationic conjugated polymers and small molecules containing bispyridinium units may be a class of high-performance materials for organic photoelectric devices and sensors.

Dibenzothiophene-*S,S*-dioxide (FSO) is a well-known n-type aromatic heterocycle that exhibits good thermal stability, high fluorescence efficiency, high electron affinity and electron-transporting ability.^{41–44} Previously, we synthesized a family of blue, green and red light-emitting polyfluorenes (PFs) containing FSO units.¹ These polymers exhibited excellent electroluminescent performance with maximal efficiencies of 7.0, 17.6 and 6.1 cd A⁻¹ for the blue, green and red light-emitting polymers, respectively. Subsequently, we introduced FSO moieties into the backbones of alcohol-soluble PFs containing amino groups.⁴⁵ When these polymers were utilized as cathode interlayers in OLEDs and OPVs, some of them displayed better modification performance than the famous interfacial material, poly[(9,9-bis(3-(*N,N*-dimethylamino)propyl)-2,7-fluorene)-*alt*-2,7-(9,9-dioctylfluorene)], which was attributed to enhancements in the electron-transporting properties of these polymers by the FSO units. In addition, we also obtained a series of novel polycyclic aromatic compounds based on FSO-fused

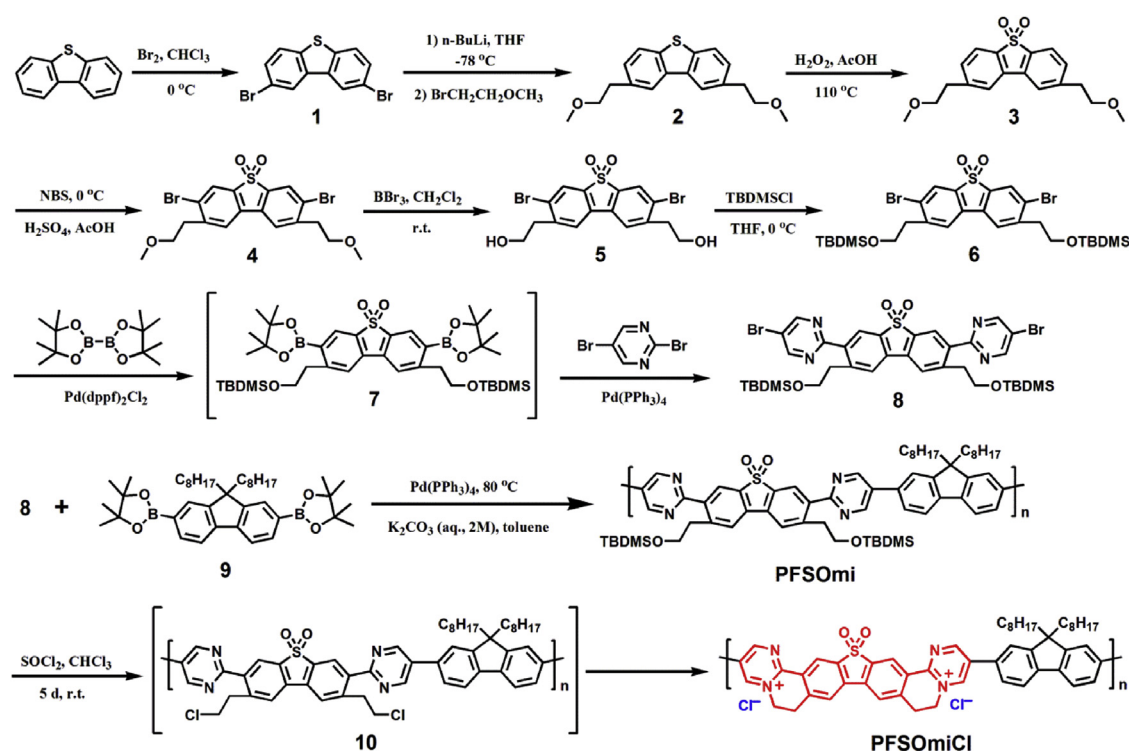
seven rings, which displayed high thermal stabilities and photoluminescence quantum yields.⁴⁶

Previously, we demonstrated the successful synthesis of two novel cationic conjugated small molecules based on bispyridinium-FSO or bispyrimidinium-FSO segments, and their photoelectronic properties were investigated in detail.⁴⁷ Herein, we report the design and synthesis of a novel n-type cationic conjugated polymer (**PFSOmiCl**), consisting of bispyrimidinium-FSO and fluorene scaffolds. The bispyrimidinium-FSO unit endows the polyelectrolyte with high electrophilicity and a planar structure for π -electron delocalization. In addition, the pyrimidinium rings offer this polymer versatile solubility and processability in highly polar solvents. The octyl group side chains within a fluorene repeating unit grant the polymer good film-forming ability. Therefore, this type of WSCP may be a potential material for organic electronic devices, such as OLEDs, OPVs, PVSCs and bio/chemosensors.

2. Results and discussion

2.1. Synthesis

The synthetic route of **PFSOmiCl** is shown in Scheme 1. Compound **1** was reacted with *n*-BuLi in anhydrous tetrahydrofuran (THF) at -78 °C, after which the reaction was quenched by 1-bromo-2-methoxyethane. Compound **3** was obtained as a white solid by oxidizing **2** with a H₂O₂ aqueous solution. Subsequently, bromination of **3** with *N*-bromobutanamide in the mixed solvent of concentrated H₂SO₄ and AcOH (3:1, v/v) offered compound **4**. It was found that the presence of concentrated H₂SO₄ was indispensable for improving the reaction yield. Compound **4** could be separated from the byproducts by column chromatography on silica gel with ethyl/petroleum (1/1, v/v) as the eluent. Then, elimination of the methyl groups within the side chains of **4** by BBr₃ generated **5**. Compound **5** has poor solubility in common organic solvents (THF, CHCl₃, toluene and so on). Compound **6** was obtained through the



Scheme 1. Synthetic routes for the monomers and polymers.

reaction between **5** and *t*-butyldimethylchlorosilane (TBDMSCl) in anhydrous THF at 0 °C. The reaction yield was as high as 92% and the solubility of **6** is much higher than that of **5**, due to the introduction of TBDMS groups. The chemical structures of compounds **1–6** were verified by ¹H NMR, ¹³C NMR (Figures S1–S6), atmospheric pressure chemical ionization mass spectrometry (APCI-MS) and elemental analysis. Intermediate **7** was obtained through the Pd-catalyzed Suzuki–Miyama coupling reaction between **6** and bis(pinacolato)diboron at 85 °C. The crude product of **7** was extracted by fast column chromatography on neutral Al₂O₃ with ethyl acetate/petroleum ether (1/1, v/v) as the eluent. It was difficult to exhaustively obtain pure **7** by further purifications, and the further purifications were accompanied by a great loss of **7**, so the crude product of **7** was used for the next step directly. Monomer **8** was prepared through the common Pd-catalyzed Suzuki cross-coupling reaction between intermediate **7** and 2,5-dibromopyrimidine, and its structure was also confirmed by ¹H NMR, ¹³C NMR (Figure S7), APCI-MS and elemental analysis. The other monomer **9**, 2,7-bis(4,4,5,5-tertramethyl-[1,3,2]-dioxaborolan-2-yl)-9,9-dioctyl-fluorene, was synthesized according to a literature procedure.⁴⁸ The copolymerization between **8** and **9** through the standard Pd-catalyzed Suzuki cross-coupling reaction afforded the precursor polymer poly[2,7-(9,9-dioctylfluorene)-*alt*-5,5-(3',7'-di-2-pyrimidinyl-2',8'-bis(2-(*tert*-butyldimethylsilyloxy)ethyl)-dibenzothiophene-*S,S*-dioxide)] (**PFSOmi**). **PFSOmi** is readily soluble in common organic solvents, such as THF and CHCl₃, but insoluble in highly polar solvents (water, DMSO, methanol and so on). Its number average molecular weight (*M_n*) tested by gel permeation chromatography (GPC) is 16900 Da, with a polydispersity index of 1.5. The conjugated polyelectrolyte (CPE), **PFSOmiCl**, was prepared from **PFSOmi** via two steps.³⁶ Firstly, **PFSOmi** was treated with SOCl₂, during which the TBDMSO groups within **PFSOmi** were substituted by chlorine atoms from SOCl₂ and thus intermediate **10** was generated. Secondly, the intramolecular nucleophilic substitution reaction of **10** took place, which finally formed the target CPE, **PFSOmiCl**. **PFSOmiCl** is readily soluble in DMSO, and partly soluble in methanol and *N,N*-dimethylformamide, but is insoluble in water and low polarity solvents such as CHCl₃, THF and toluene. This unique solubility endows **PFSOmiCl** with excellent application potential as a cathode interlayer in solution-processed multilayer OLEDs, OPVs and PVSCs, since the adjacent layers are usually deposited from low-polarity solvents.²⁹

The ¹H NMR spectra of **PFSOmi** and **PFSOmiCl** agree with their chemical structures, as shown in Figures S8 and S9. The signals of the protons adjacent to the nitrogen atoms are located at 9.19 ppm in the spectrum of **PFSOmi**. Whereas the responses of the protons adjacent to the nitrogen cations or nitrogen atoms shift to 10.26 or 10.14 ppm, respectively, in the spectrum of **PFSOmiCl**, due to the generation of electron-withdrawing N⁺ cations. The signals of the other protons within the aromatic rings of **PFSOmiCl** also possess higher chemical shifts compared to those of **PFSOmi**. The resonances at 3.68 and 5.13 ppm are induced by the protons within the ethylene bridges in the spectrum of **PFSOmiCl**. The intense peaks at about 0.91 and 0.02 ppm, which are induced by the TBDMS groups, disappear in the spectrum of **PFSOmiCl**. These results indicate that the CPE could be readily prepared from its precursor.

2.2. Thermal properties

The thermal properties of **PFSOmiCl** were investigated by thermo-gravimetric analysis (TGA). The results are shown in Fig. 1. The scanning temperatures were ramped from 50 to 800 °C with a consistent increasing rate of 10 °C min⁻¹. **PFSOmiCl** exhibits two main degradation processes that probably result from the cleavage of octyl groups and ethylene bridges, and the onset temperature of

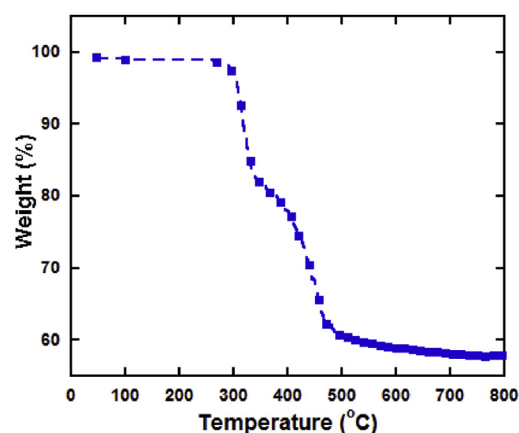


Fig. 1. Thermo-gravimetric analysis curve of **PFSOmiCl**.

decomposition process is about 293 °C. The results imply good thermal stability of **PFSOmiCl**.

2.3. Optical properties

The UV–vis absorption and photoluminescence (PL) spectra of **PFSOmi** and **PFSOmiCl** in solution and film form are shown in Fig. 2, and the details of the optical properties are summarized in Table 1. As shown in Fig. 2(a), **PFSOmi** exhibits a single absorption peak at 375 nm in THF solution, and a bathochromal band at 394 nm in film state. Alternatively, the absorption spectrum of **PFSOmiCl** in DMSO shows a slight band at about 346 nm, which

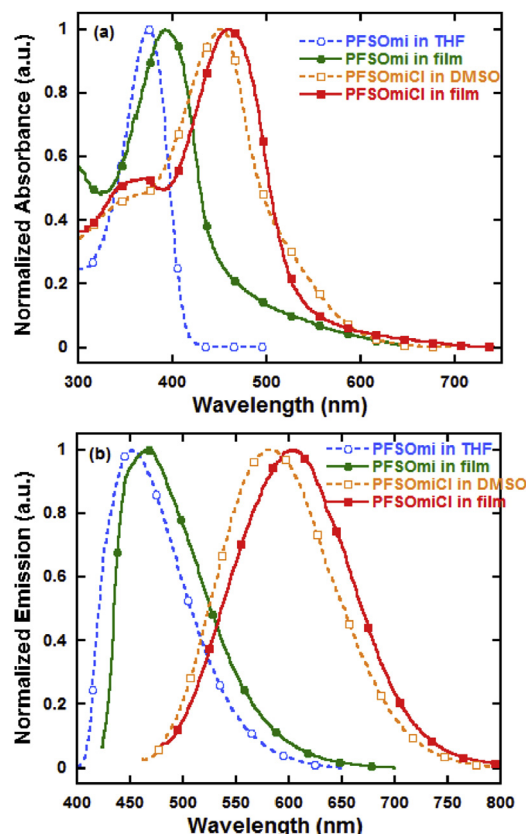


Fig. 2. UV–vis absorption (a) and PL (b) spectra of **PFSOmi** and **PFSOmiCl**.

Table 1
UV–vis absorption and PL properties of **PFSOmi** and **PFSOmiCl**.

Polymer	λ_{abs} (nm)		λ_{PL} (nm)		$E_{\text{g}}^{\text{opt}}$ (eV)
	Solution	Film	Solution	Film	
PFSOmi	375	394	451	468	2.80
PFSOmiCl	346	363	583	604	2.33
	453	460			

can be attributed to the π - π^* transition of the conjugated backbone, and an intense peak at about 453 nm that results from the intramolecular charge-transfer (ICT) effect. The absorption peaks of **PFSOmiCl** in film bathochromically shift to 363 and 460 nm, due to the intermolecular aggregation in the solid film state. It is interesting to note that the absorption spectra of **PFSOmiCl** are obviously red-shifted compared with those of **PFSOmi** in both solution and film form. This is because the newly formed ethylene bridges enforce the planar conformation of the bispyrimidinium-FSO scaffold, which decreases the torsion angles between pyrimidinium and FSO rings, and thus enhances the molecular orbital overlap, as well as the delocalization of electrons.^{36,49} In addition, the formation of pyrimidinium salts can improve the electron-withdrawing ability of the bispyrimidinium-FSO segment, and thus promote the ICT within conjugated backbones and decrease the band gap of **PFSOmiCl**.^{37,50} The optical band gaps ($E_{\text{g}}^{\text{opt}}$ s) of **PFSOmi** and **PFSOmiCl**, calculated from the absorption onsets in films, are 2.80 and 2.33 eV, respectively.

In order to achieve a more insightful understanding of the optical properties of **PFSOmi** and **PFSOmiCl**, their PL spectra were also recorded in both solution and film form, as shown in Fig. 2(b). **PFSOmi** displays emission peaks at 451 and 468 nm in solution and film form, respectively. The locations of the PL peaks of **PFSOmiCl** bathochromically shift to 583 and 604 nm in DMSO and film, respectively. Similarly, the reason for the red shifts of PL spectra can be assigned to the more planar conformation and stronger ICT of **PFSOmiCl** compared with **PFSOmi**. Moreover, relative to **PFSOmi**, **PFSOmiCl** reveals broader PL spectra in both solution and film form that is also due to the stronger ICT effect in **PFSOmiCl**.³⁹

2.4. Electrochemical properties

Cyclic voltammetry (CV) was used to investigate the electrochemical properties of **PFSOmi** and **PFSOmiCl**. The results are shown in Fig. 3 and Table 2. The redox potential ($E_{1/2}$) of ferrocene/

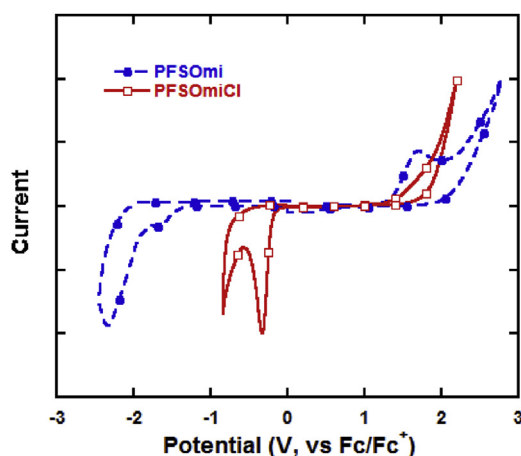


Fig. 3. Cyclic voltammogram of **PFSOmiCl** in film measured in 0.1 M Bu₄NPF₆ in acetonitrile at a scan rate of 50 mV s⁻¹.

Table 2
Electrochemical properties of **PFSOmi** and **PFSOmiCl**.

Polymer	E_{red} (V)	E_{ox} (V)	LUMO (eV)	HOMO (eV)	E_{g}^{a} (eV)
PFSOmi	-1.41	1.35	-2.98	-5.74	2.76
PFSOmiCl	-0.21	1.42	-4.18	-5.81	1.63

^a $E_{\text{g}} = \text{LUMO} - \text{HOMO}$.

ferrocenium (Fc/Fc⁺) was measured to be 0.41 V using a SCE reference electrode under the same experimental conditions. Since the redox potential of Fc/Fc⁺ has an absolute energy level of -4.80 eV to the vacuum energy level,⁵¹ the highest occupied molecular orbital (HOMO) and the lowest unoccupied molecular orbital (LUMO) energy levels can be calculated according to the empirical equations: HOMO = -e($E_{\text{ox}} + 4.8 - 0.41$) (eV), LUMO = -e($E_{\text{red}} + 4.8 - 0.41$) (eV), where E_{ox} and E_{red} are the onset oxidation and reduction potential vs. SCE, respectively. As shown in Fig. 3 and Table 2, **PFSOmi** exhibits E_{red} and E_{ox} values of about -1.41 and 1.35 V, respectively, and the LUMO and HOMO energy levels are thus -2.98 and -5.74 eV, respectively. For **PFSOmiCl**, the reduction onset at about -0.29 V is attributed to the reduction of one of the N⁺ cations,³⁶ and the more negative reduction band is caused by the reduction of H₂O within the testing system, as observed in our blank test under the same conditions. In addition, the oxidation behavior at the positive voltage side is ascribed to the oxidation of the fluorene unit.²⁶ The E_{red} and E_{ox} values of **PFSOmiCl** are located at -0.21 and 1.42 V, respectively, so the LUMO and HOMO energy levels are about -4.18 and -5.81 eV, respectively. Note that in comparison with **PFSOmi**, **PFSOmiCl** shows deeper LUMO and HOMO levels, which is attributed to the introduction of electron-withdrawing pyrimidinium salts.⁵² Furthermore, it is well known that in a donor-acceptor (D-A) copolymer, the HOMO level of the copolymer mainly depends on the D unit, and the LUMO level is mainly related to the A unit.⁵² Since **PFSOmi** and **PFSOmiCl** own the same D units (fluorene), their HOMO levels are close to each other, but their A units (bispyrimidinium-FSO) are distinctly different, which results in the significant difference in their LUMO levels. Moreover, it is interesting to note that the LUMO energy level of **PFSOmiCl** is very close to the LUMO energy levels of common fullerene derivatives, such as [6,6]-phenyl-C₆₁-butyric acid methyl ester and [6,6]-phenyl-C₇₀-butyric acid methyl ester (in the range of -3.8 to -4.3 eV),^{53–55} which suggests that **PFSOmiCl** can form an ohmic contact with these fullerene derivatives, and this is helpful for electron transportation and extraction when **PFSOmiCl** is applied as cathode modification layer in OPVs or PVSCs.³⁵ Moreover, the relatively deep-lying HOMO energy level is able to prevent hole carriers from flowing towards the cathode, which can improve the performance of OLEDs, OPVs and PVSCs.¹⁶

2.5. Wetting properties

The wetting properties of the precursor polymer and poly-electrolyte were estimated by measuring the water contact angle (θ) on each surface of the **PFSOmi** and **PFSOmiCl** films, and the images were recorded with a digital camera. As shown in Fig. 4, the θ value of **PFSOmi** film is 103.6°, yet the surface of **PFSOmiCl** layer becomes more hydrophilic with a θ of 87.0°. This is probably due to the accumulation of the ionic components in the topmost surface of **PFSOmiCl** film, as observed for other CPE films.⁵⁶ It was reported that in OPV devices, when covered with a perylene diimide-based cathode interlayer containing phosphate groups (PDIP), the active layer became more hydrophilic with a decreased θ , which eased the inherent incompatibility between the metal cathode and organic layer.⁵⁷ They found that the improved wettability of the active layer

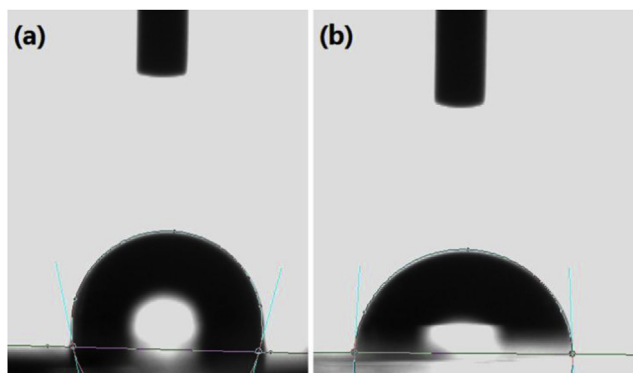


Fig. 4. Water contact angle images of PFSOmi (a) and PFSOmiCl (b) layers.

with cathode by PDIP could reduce the contact resistance and thus improve the OPV performance. Similarly, the increased hydrophilicity of organic light-emitting layers in OLEDs and organic electron-transporting layers in PVSCs by cathode interlayers could also optimize the compatibility between organic layers and metal cathodes, and thus improve the device performance.^{58,59} Therefore, when PFSOmiCl is employed as a cathode interlayer in OPVs, OLEDs or PVSCs, its hydrophilic surface is expected to improve the wettability of organic layer with inorganic cathode that is important for reducing the contact resistance and increasing the device performance.

3. Conclusions

A novel n-type cationic conjugated polymer (PFSOmiCl) composed of bispyrimidinium-FSO and fluorene building blocks has been designed and synthesized. In comparison with its polymeric precursor (PFSOmi), PFSOmiCl shows distinctive optical and wetting properties as a result of the generation of electron-deficient pyrimidinium salts. In both solution and film form, PFSOmiCl exhibits significantly bathochromical UV–vis absorption and PL spectra, as well as broader PL bands, when compared with PFSOmi. The hydrophilic and wetting properties of the PFSOmiCl film are also dramatically better than those of the PFSOmi film. Moreover, PFSOmiCl displays a deep-lying LUMO energy level of -4.18 eV that is comparable to the LUMO energy levels of common fullerene derivatives, which means the probable formation of ohmic contact at the PFSOmiCl/fullerene interface in OPVs and PVSCs. These unique features including good thermal stability, polar-solvents solubility, nice hydrophilicity, high electron affinity and large conjugated plane signify that PFSOmiCl may be a promising material candidate for organic electronic applications.

4. Experimental section

4.1. General procedures

All reagents, unless otherwise specified, were purchased from Aladdin Chemical Co., Sigma Aldrich Chemical Co., Alfa Aesar Chemical Co. or J&K Chemical Co., and were used as received. Anhydrous THF and toluene used for polymerization were further purified by normal procedures and distilled before used. All air and water sensitive synthetic manipulations were performed under dry argon or nitrogen atmosphere.

^1H NMR and ^{13}C NMR measurements were carried out on a Bruker AV-300 spectrometer operating at 300 MHz (for ^1H) and 75 MHz (for ^{13}C) with tetramethylsilane (TMS) as the internal reference. APCI-MS analyses were obtained from an Acquity Waters

UPLC equipped with Waters Acquity TQ detector (Thermo Finnigan LCQ Fleet system). Elemental analyses were performed on a Vario EL elemental analysis instrument (Elementar Co.). Molecular weight of the precursor polymer was determined by a Waters GPC 2410 in THF using a calibration curve with polystyrene standards. Thermo-gravimetric analysis (TGA) was conducted using a NETZSCH TG 209 at a heating rate of $10\text{ }^\circ\text{C min}^{-1}$ and a nitrogen flow rate of 20 mL min^{-1} . UV–vis absorption spectra were performed on a HP 8453 spectrophotometer. PL spectra were recorded on an Instaspec IV CCD spectrophotometer (Oriel Co.). Cyclic voltammetry (CV) were characterized on a CHI600D electrochemical workstation with a standard three electrodes cell based on a Pt wire counter electrode and a platinum (Pt) working electrode, against saturated calomel electrode (SCE) as reference electrode at a scan rate of 50 mV s^{-1} within a nitrogen-saturated anhydrous solution of 0.1 mol L^{-1} tetrabutylammonium hexafluorophosphates (Bu_4NPF_6) in acetonitrile, versus ferrocene/ferrocenium (Fc/Fc^+) as the internal reference.

4.2. Synthetic procedures

4.2.1. 2,8-Dibromo-dibenzothiophene (1)

Into a mixture of dibenzothiophene (50.0 g, 272 mmol), Fe (1.00 g, 18.0 mmol) and CHCl_3 (400 mL) was added Br_2 (35.0 mL, 680 mmol) (diluted with CHCl_3 (100 mL)) slowly at $0\text{ }^\circ\text{C}$. The mixture was gradually warmed to room temperature with vigorously stirring overnight. Then aqueous solution of NaHSO_3 (28.3 g, 272 mmol) was added to quench the reaction. The mixture was filtered, and the residue was washed with water and purified by recrystallization from THF to afford **1** as a white crystal (39.0 g, 41.9%). ^1H NMR (300 MHz, CDCl_3) δ (ppm): 8.23 (d, $J = 1.8$ Hz, 2H), 7.72–7.69 (d, $J = 8.4$ Hz, 2H), 7.59–7.56 (dd, $J = 8.4$ Hz, $J = 2.0$ Hz, 2H). ^{13}C NMR (75 MHz, CDCl_3) δ (ppm): 138.75, 136.30, 130.43, 124.86, 124.33, 118.76. MS (APCI) calculated for $\text{C}_{12}\text{H}_6\text{Br}_2\text{S}$: 342.1, found: 343.0. Elemental analysis calculated for $\text{C}_{12}\text{H}_6\text{Br}_2\text{S}$: C, 42.14; H, 1.77; S, 9.37, found: C, 41.62; H, 1.99; S, 9.86.

4.2.2. 2,8-Bis(2-methoxyethyl)-dibenzothiophene (2)

Into the solution of **1** (3.42 g, 10.0 mmol) in anhydrous THF (200 mL) was slowly added n-BuLi (2.4 M in n-hexane, 10.4 mL) at $-78\text{ }^\circ\text{C}$ under argon, and the reaction mixture was stirred at $-78\text{ }^\circ\text{C}$ for 1 h followed by quenching with 1-bromo-2-methoxyethane (2.80 mL, 30.0 mmol). The solution was then freely warmed to room temperature and stirred overnight. Distilled water (50 mL) was added slowly and the aqueous layer was extracted with CH_2Cl_2 for three times. The combined organic layer was washed with brine before dried over anhydrous MgSO_4 . The crude product was collected by evaporating off the solvent and then purified by column chromatography on silica gel with CH_2Cl_2 /petroleum ether (1/1, v/v) as eluent to afford **2** as a colorless oil (975 mg, 32.5%). ^1H NMR (300 MHz, CDCl_3) δ (ppm): 8.02 (s, 2H), 7.77–7.74 (d, $J = 8.1$ Hz, 2H), 7.33–7.30 (dd, $J = 8.1$ Hz, $J = 1.2$ Hz, 2H), 3.73–3.68 (t, $J = 6.9$ Hz, 4H), 3.41 (s, 6H), 3.10–3.05 (t, $J = 6.9$ Hz, 4H). ^{13}C NMR (75 MHz, CDCl_3) δ (ppm): 137.77, 135.71, 135.32, 127.82, 122.70, 121.81, 73.94, 58.81, 36.35. MS (APCI) calculated for $\text{C}_{18}\text{H}_{20}\text{O}_2\text{S}$: 300.4, found: 301.0. Elemental analysis calculated for $\text{C}_{18}\text{H}_{20}\text{O}_2\text{S}$: C, 71.96; H, 6.71; S, 10.67, found: C, 71.54; H, 6.95; S, 10.55.

4.2.3. 2,8-Bis(2-methoxyethyl)-dibenzothiophene-S,S-dioxide (3)

30% aqueous solution of H_2O_2 (10.0 mL, 88.2 mmol) was added into the solution of **2** (1.40 g, 4.67 mmol) in AcOH (35 mL) at $110\text{ }^\circ\text{C}$ and the reaction was refluxed for 5 h. After cooled to room temperature, the mixture was poured into distilled water with vigorously stirring. The precipitate was then collected and father

purified by column chromatography on silica gel with ethyl acetate/petroleum ether (1/1, *v/v*) as eluent to afford **3** as a white solid (1.32 g, 85.5%). ¹H NMR (300 MHz, CDCl₃) δ (ppm): 7.74–7.71 (d, *J* = 7.8 Hz, 2H), 7.65–7.64 (d, *J* = 0.6 Hz, 2H), 7.38–7.35 (dd, *J* = 7.8 Hz, *J* = 1.2 Hz, 2H), 3.68–3.63 (t, *J* = 6.5 Hz, 4H), 3.36 (s, 6H), 3.01–2.96 (t, *J* = 6.6 Hz, 4H). ¹³C NMR (75 MHz, CDCl₃) δ (ppm): 146.25, 136.25, 132.08, 130.95, 122.24, 122.18, 72.85, 58.97, 36.59. MS (APCI) calculated for C₁₈H₂₀O₄S: 332.4, found: 333.5. Elemental analysis calculated for C₁₈H₂₀O₄S: C, 65.04; H, 6.06; S, 9.65, found: C, 65.48; H, 6.29; S, 9.32.

4.2.4. 3,7-Dibromo-2,8-bis(2-methoxyethyl)-dibenzothiophene-S,S-dioxide (**4**)

Into the mixture of **3** (3.32 g, 10.0 mmol), H₂SO₄ (90 mL) and AcOH (30 mL) was added *N*-bromosuccinimide (3.91 g, 22.0 mmol) slowly at 0 °C in the absence of light. Then the reaction was allowed to warm to room temperature and stirred overnight. After the reaction mixture was poured slowly into ice water, the mixture was filtered and the precipitate was purified by column chromatography on silica gel with ethyl acetate/petroleum ether (1/1, *v/v*) as eluent to afford **4** as a white solid (3.50 g, 71.2%). ¹H NMR (300 MHz, CDCl₃) δ (ppm): 7.94 (s, 2H), 7.68 (s, 2H), 3.69–3.65 (t, *J* = 6 Hz, 4H), 3.37 (s, 6H), 3.15–3.10 (t, *J* = 7.5 Hz, 4H). ¹³C NMR (75 MHz, CDCl₃) δ (ppm): 145.41, 137.15, 130.20, 126.61, 126.39, 124.25, 70.91, 59.02, 37.13. MS (APCI) calculated for C₁₈H₁₈Br₂O₄S: 490.2, found: 491.6. Elemental analysis calculated for C₁₈H₁₈Br₂O₄S: C, 44.10; H, 3.70; S, 6.54, found: C, 43.81; H, 3.99; S, 6.29.

4.2.5. 3,7-Dibromo-2,8-bis(2-hydroxyethyl)-dibenzothiophene-S,S-dioxide (**5**)

In the absence of light, BBr₃ (4.80 mL, 50.0 mmol) was dropped slowly into the mixture of CH₂Cl₂ (200 mL) and **4** (4.90 g, 10.0 mmol) at room temperature. After stirred overnight, the reaction was quenched with distilled water (10 mL) slowly. The solvent was evaporated off and ethyl acetate was added to solve the solid. The organic layer was washed with dilute aqueous solution of NaOH and brine before dried over anhydrous MgSO₄. The crude product was collected by evaporating off the solvent and purified by column chromatography on silica gel with ethyl acetate/petroleum ether (5/1, *v/v*) as eluent to afford **5** as a white solid (3.99 g, 86.4%). ¹H NMR (300 MHz, DMSO-*d*₆) δ (ppm): 8.30 (s, 2H), 8.19 (s, 2H), 4.95–4.92 (t, *J* = 5.3 Hz, 2H), 3.75–3.68 (m, 4H), 3.02–2.97 (t, *J* = 6.6 Hz, 4H). ¹³C NMR (75 MHz, DMSO-*d*₆) δ (ppm): 145.87, 136.33, 129.45, 126.07, 126.00, 125.23, 59.69, 59.58. MS (APCI) calculated for C₁₆H₁₄Br₂O₄S: 462.2, found: 463.4. Elemental analysis calculated for C₁₆H₁₄Br₂O₄S: C, 41.58; H, 3.05; S, 6.94, found: C, 41.03; H, 3.77; S, 6.12.

4.2.6. 3,7-Dibromo-2,8-bis[2-(*tert*-butyldimethylsilyloxy)ethyl]-dibenzothiophene-S,S-dioxide (**6**)

T-butyldimethylchlorosilane (TBDMSCl) (3.91 g, 25.9 mmol) was added in one portion into the mixture of **5** (5.00 g, 10.8 mmol), anhydrous THF (200 mL) and imidazole (2.21 g, 32.4 mmol) at 0 °C under argon. After stirring overnight, 200 mL of water was added into the mixture. Then the aqueous layer was extracted with ethyl acetate for three times. The combined organic layer was washed with brine before dried over anhydrous MgSO₄. The solution was concentrated and the crude product was further purified by column chromatography on silica gel with ethyl acetate/petroleum ether (1/5, *v/v*) as eluent to afford **6** as a white solid (6.83 g, 91.5%). ¹H NMR (300 MHz, CDCl₃) δ (ppm): 7.95 (s, 2H), 7.67 (s, 2H), 3.90–3.85 (t, *J* = 6.5 Hz, 4H), 3.10–3.05 (t, *J* = 6.3 Hz, 4H), 0.86 (s, 18H), –0.02 (s, 12H). ¹³C NMR (75 MHz, CDCl₃) δ (ppm): 145.60, 137.10, 129.90, 126.54, 126.41, 124.44, 61.69, 40.04, 26.00, 18.36, –5.30. MS (APCI) calculated for C₂₈H₄₂Br₂O₄SSi₂: 690.7, found: 691.8. Elemental

analysis calculated for C₂₈H₄₂Br₂O₄SSi₂: C, 48.69; H, 6.13; S, 4.64, found: C, 48.03; H, 6.49; S, 4.98.

4.2.7. 3,7-Bis(4,4,5,5-tetramethyl-1,3,2-dioxaborolan-2-yl)-2,8-bis[2-(*tert*-butyldimethylsilyloxy)ethyl]-dibenzothiophene-S,S-dioxide (**7**)

6 (5.00 g, 7.23 mmol), AcOK (4.96 g, 50.6 mmol) and 4,4,5,5,4',4',5',5'-octamethyl-[2,2']bi[[1,3,2]dioxaborolanyl] (5.51 g, 21.7 mmol) were mixed with Pd(dppf)Cl₂ (0.16 g, 0.2 mmol) in 1,4-dioxane (100 mL) under argon. Then the reaction mixture was stirred at 85 °C overnight under argon. Distilled water was poured into the reaction after cooled to room temperature. Ethyl acetate was used to extract the aqueous layer for three times. The combined organic layer was washed with brine before dried over anhydrous MgSO₄. Then the solvent was evaporated off and the crude product was gotten by fast column chromatography on Al₂O₃ using ethyl acetate/petroleum ether (1/1, *v/v*) as eluent. The crude product was used to synthesize **8** without further purification. MS (APCI) calculated for C₄₀H₆₆B₂O₈SSi₂: 784.8, found: 785.5.

4.2.8. 3,7-Bis(5-bromopyrimidin-2-yl)-2,8-bis[2-(*tert*-butyldimethylsilyloxy)ethyl]-dibenzothiophene-S,S-dioxide (**8**)

The crude product **7** (1.00 g), 2,5-dibromopyrimidine (730 mg, 3.10 mmol), TBAB (30 mg), toluene (15 mL), aqueous solution of K₂CO₃ (2 M, 4.00 mL) and Pd(PPh₃)₄ (45.0 mg, 0.0400 mmol) were added into a 50 mL of three-neck flask under argon. The reaction was heated to 85 °C and stirred overnight. Then the reaction was cooled to room temperature and mixed with distilled water (35 mL). The aqueous layer was extracted with ethyl acetate for three times. The combined organic layer was washed with distilled water and brine before dried over anhydrous MgSO₄. The organic solvent was distilled and the crude product was purified by column chromatography with ethyl acetate/petroleum ether (1/1, *v/v*) as eluent to afford **8** as a white solid (500 mg). ¹H NMR (300 MHz, CDCl₃) δ (ppm): 8.92 (s, 4H), 8.47 (s, 2H), 7.85 (s, 2H), 3.93–3.91 (t, *J* = 3 Hz, 4H), 3.35–3.32 (t, *J* = 4.5 Hz, 4H), 0.87 (s, 18H), –0.03 (s, 12H). ¹³C NMR (75 MHz, CDCl₃) δ (ppm): 163.41, 157.83, 145.72, 138.96, 136.82, 131.54, 125.59, 125.21, 119.08, 63.68, 37.82, 25.94, 18.30, –5.37. MS (APCI) calculated for C₃₆H₄₆Br₂N₄O₄SSi₂: 846.8, found: 847.4. Elemental analysis calculated for C₃₆H₄₆Br₂N₄O₄SSi₂: C, 51.06; H, 5.48; N, 6.62; S, 3.79, found: C, 51.68; H, 5.99; N, 6.36; S, 3.52.

4.2.9. Poly[2,7-(9,9-dioctylfluorene)-alt-5,5-(3',7'-di-2-pyrimidinyl-2',8'-bis(2-(*tert*-butyldimethylsilyloxy)ethyl)-dibenzothiophene-S,S-dioxide)] (**PFSoMi**)

Monomer **8** (169.0 mg, 0.2000 mmol), 2,7-bis(4,4,5,5-tetramethyl-1,3,2-dioxaborolan-2-yl)-9,9-dioctyl-fluorene (**9**) (128.5 mg, 0.2000 mmol), toluene (7.0 mL), aqueous solution of K₂CO₃ (2 M, 0.50 mL) and Pd(PPh₃)₄ (8.0 mg) were mixed in a 50 mL of two-neck flask under argon protection. The reaction was stirred at 80 °C for 24 h under argon atmosphere. After cooled to room temperature, the mixture was poured into methanol (200 mL). The precipitate was collected by filtration and then washed with methanol and acetone successively in a Soxhlet. The obtained solid was dissolved in THF (8 mL) and filtered through a 0.45 μm polytetrafluoroethylene (PTFE) filter. The solution was concentrated followed by precipitation from methanol (150 mL) to get the target polymer (179.0 mg, 83%). ¹H NMR (300 MHz, CDCl₃) δ (ppm): 9.19 (s, 4H), 8.60 (s, 2H), 7.95 (br, 2H), 7.91–7.68 (m, 6H), 4.02 (br, 4H), 3.46 (br, 4H), 2.27–1.99 (m, 4H), 1.25–0.79 (m, 48H), 0.02 (s, 12H). Elemental analysis calculated for C₆₅H₈₆N₄O₄SSi₂: C, 72.58; H, 8.06; N, 5.21; S, 2.98, found: C, 71.93; H, 8.42; N, 5.44; S, 2.75. GPC (THF, polystyrene standard) analysis showed a *M_n* = 16900 and *PDI* = 1.514.

4.2.10. The polyelectrolyte (PFSomiCl)

SOCl₂ (2.0 mL) was added into the mixture of PFSomi (80 mg, 0.074 mmol) and CHCl₃ (9 mL) under argon. The reaction was vigorously stirred at room temperature for 5 days. The solution was evaporated, and the resulting solid was dissolved in DMSO (3 mL), and then precipitated from ethyl acetate (100 mL). The collected precipitate by filtration was washed with THF and acetone successively in a Soxhlet to give PFSomiCl as a red solid (59 mg, 90%). ¹H NMR (300 MHz, DMSO-*d*₆) δ (ppm): 10.26 (br, 2H), 10.14 (br, 2H), 8.98 (s, 2H), 8.69 (br, 2H), 8.47–8.09 (m, 6H), 5.13 (br, 4H), 3.68 (br, 4H), 2.27–1.97 (m, 4H), 1.23–0.75 (m, 30H). Elemental analysis calculated for C₅₃H₅₆Cl₂N₄O₂S: C, 72.01; H, 6.39; N, 6.34; S, 3.63, found: C, 71.53; H, 7.00; N, 6.82; S, 3.41.

Acknowledgements

This work was financially supported by the National Nature Science Foundation of China (nos. 51273069, 91333206), General Financial Grant from the China Postdoctoral Science Foundation (no. 2015M582409) and Shenzhen Fundamental R&D Program (no. JCYJ20160520175355048).

Appendix A. Supplementary data

Supplementary data related to this article can be found at <http://dx.doi.org/10.1016/j.tet.2017.03.062>.

References

- Yu L, Liu J, Hu S-J, et al. *Adv Funct Mater.* 2013;23:4366–4376.
- Grimsdale AC, Chan KL, Martin RE, Jokisz PG, Holmes AB. *Chem Rev.* 2009;109:897–1091.
- Liu J, Li L, Pei Q-B. *Macromolecules.* 2011;44:2451–2456.
- He Z, Zhong C, Su S, Xu M, Wu H, Cao Y. *Nat Photonics.* 2012;6:591–595.
- Li Y-F. *Acc Chem Res.* 2012;45:723–733.
- He Z, Xiao B, Liu F, et al. *Nat Photonics.* 2015;9:174–179.
- Allard S, Forster M, Souharce B, Thiem H, Scherf U. *Angew Chem Int Ed.* 2008;47:4070–4098.
- Wang C, Dong H, Hu W, Liu Y, Zhu D. *Chem Rev.* 2012;112:2208–2267.
- Yang L, Xiao C-Y, Jiang W, Wang Z-H. *Tetrahedron.* 2014;70:6265–6270.
- Swager TM. *Acc Chem Res.* 1998;31:201–207.
- Feng X, Liu L, Wang S, Zhu D. *Chem Soc Rev.* 2010;39:2411–2419.
- Usta H, Lu G, Facchetti A, Marks TJ. *J Am Chem Soc.* 2006;128:9034–9035.
- He Z-C, Zhang C, Xu X-F, et al. *Adv Mater.* 2011;23:3086–3089.
- Heywang G, Jonas F. *Adv Mater.* 1992;4:116–118.
- Zhao R-Y, Dou C-D, Xie Z-Y, Liu J, Wang L-X. *Angew Chem Int Ed.* 2016;55:5313–5317.
- Sun C, Wu Z-H, Yip H-L, et al. *Adv Energy Mater.* 2016;6:1501534.
- Li C, Zhang A-D, Wang Z-W, et al. *RSC Adv.* 2016;6:35677–35683.
- Chirvase D, Parisi J, Hummelen JC, Dyakonov V. *Nanotechnology.* 2004;15:1317–1323.
- Feng L, Li H, Qu Y, Lu C. *Chem Commun.* 2012;48:4633–4635.
- He G, Yan N, Yang J, et al. *Macromolecules.* 2011;44:4759–4766.
- Yang J-S, Swager TM. *J Am Chem Soc.* 1998;120:11864–11873.
- Sanchez JC, Troglor WC. *J Mater Chem.* 2008;18:3143–3156.
- Kim Y, Whitten JE, Swager TM. *J Am Chem Soc.* 2005;127:12122–12130.
- Rochat S, Swager TM. *J Am Chem Soc.* 2013;135:17703–17706.
- Rochat S, Swager TM. *Angew Chem Int Ed.* 2014;53:9792–9796.
- Huang F, Wu H-B, Wang D-L, Yang W, Cao Y. *Chem Mater.* 2004;16:708–716.
- Huang F, Wu H-B, Cao Y. *Chem Soc Rev.* 2010;39:2500–2521.
- Duan C-H, Zhang K, Zhong C-M, Huang F, Cao Y. *Chem Soc Rev.* 2013;42:9071–9104.
- Hu Z-C, Zhang K, Huang F, Cao Y. *Chem Commun.* 2015;51:5572–5585.
- Feng X-L, Liu L-B, Wang S, Zhu D-B. *Chem Soc Rev.* 2010;39:2411–2419.
- Xu W-D, Yan C-F, Kan Z-P, Wang Y, Lai W-Y, Huang W. *ACS Appl Mater Interface.* 2016;8:14293–14300.
- Chen W-W, Jiao W-X, Li D-B, et al. *Chem Mater.* 2016;28:1227–1235.
- Xu B-W, Zheng Z, Zhao K, Hou J-H. *Adv Mater.* 2016;28:434–439.
- Zhao Y, Xie Z-Y, Qin C-J, Qu Y, Geng Y-H, Wang L-X. *Sol Energy Mater Sol Cells.* 2009;93:604–608.
- Wu Z-H, Sun C, Dong S, et al. *J Am Chem Soc.* 2016;138:2004–2013.
- Izuhara D, Swager TM. *J Am Chem Soc.* 2009;131:17724–17725.
- Izuhara D, Swager TM. *J Mater Chem.* 2011;21:3579–3584.
- Izuhara D, Swager TM. *Macromolecules.* 2011;44:2678–2684.
- Ye H, Hu X-W, Jiang Z-X, et al. *J Mater Chem A.* 2013;1:3387–3394.
- Jo M-Y, Ha Y-E, Kim JH. *Sol Energy Mater Sol Cells.* 2012;107:1–8.
- Li Y-Y, Wu H-B, Zou J-H, Ying L, Yang W, Cao Y. *Organ Electron.* 2009;10:901–909.
- Perepichka II, Perepichka IF, Bryce MR, Palsson LO. *Chem Commun.* 2005;27:3397–3399.
- Xiao H-P, Yu L, Li Y-H, et al. *Polymer.* 2012;53:2873–2883.
- Huang T-H, Whang W-T, Shen J-Y, et al. *Adv Funct Mater.* 2006;16:1449–1456.
- Xiao H-P, Miao J-S, Cao J-Q, Yang W, Wu H-B, Cao Y. *Org Electron.* 2014;15:758–774.
- Yang Y, Liang J-F, Hu L-W, Zhang B, Yang W. *New J Chem.* 2015;39:6513–6521.
- Chen G, He R, Yang W, Zhang B. *New J Chem.* 2017;41:1696–1703.
- Ranger M, Rondeau D, Leclerc M. *Macromolecules.* 1997;30:7686–7690.
- Schroeder BC, Huang ZG, Ashraf RS, et al. *Adv Funct Mater.* 2012;22:1663–1670.
- Kroon R, Gehlhaar R, Steckler TT, et al. *Sol Energy Mater Sol Cells.* 2012;105:280–286.
- Pommerehne J, Vestweber H, Guss W, et al. *Adv Mater.* 1995;7:551–554.
- Li Y. *Acc Chem Res.* 2012;45:723–733.
- Hu L, Wu F, Li C, et al. *Macromolecules.* 2015;48:5578–5586.
- Zhang Z-G, Qi B-Y, Jin Z-W, et al. *Energy Environ Sci.* 2014;7:1966–1973.
- Li C-Z, Chueh C-C, Yip H-L, O'Malley KM, Chen W-C, Jen AK-Y. *J Mater Chem.* 2012;22:8574–8578.
- Park J, Yang R, Hoven CV, et al. *Adv Mater.* 2008;20:2491–2496.
- Li M, Lv J, Wang L, et al. *Colloids Surf A Physicochem Eng Aspects.* 2015;469:326–332.
- Duan C, Wang L, Zhang K, Guan X, Huang F. *Adv Mater.* 2011;23:1665–1669.
- Zhang H, Azimi H, Hou Y, et al. *Chem Mater.* 2014;26:5190–5193.